

Electrode Characteristics and Lithiation Mechanism of FePc/GN Composites

Haoqi Yang¹, Pinchao Fan¹, Shuwu Liu¹, Junhua Wei^{2,3*}, Siping Tan^{2,3},
Qingjie Wang^{2,3} and Haoqing Hou^{1*}

¹ Department of Chemistry and Chemical Engineering, Jiangxi Normal University, Nanchang, 330022, China.

² Guizhou Meiling Battery Co., Ltd, Zunyi, 563003, China

³ State Key Laboratory of Advanced Chemical Power Sources

*E-mail: haoqing@jxnu.edu.cn (H. Hou); junhuawei09@163.com (J. Wei)

Received: 15 November 2017 / Accepted: 10 January 2018 / Published: 5 February 2018

Iron-phthalocyanine (FePc), a metal-organic compound containing a large π -conjugated and planar multi-ring aromatic structure, can be employed as an organic anode material for lithium-ion batteries. To overcome the poor electronic conductivity of FePc, a good electrically conductive graphene nanosheet carbon skeleton is integrated by a one-step simple mechanical mixing strategy. In addition, the weight ratio of FePc and graphene nanosheets (GNs) is systematically optimized. Electrochemical tests show that the as-prepared 1/2.25-FePc/GN composite exhibits a high reversible capacity of 872 mAh g⁻¹, the specific capacity based on iron-phthalocyanine is up to 1614 mAh g⁻¹. The excellent electrochemical performance of FePc/GN is mainly attributed to the synergistic effect of FePc (large π -conjugated structure, rich in N atoms and aromatic rings) and graphene (flexibility and good electrical conductivity).

Keywords: Iron-phthalocyanine; Energy storage; Organic electrode material; Lithium-ion batteries

1. INTRODUCTION

Rechargeable lithium-ion batteries (LIBs) are widely used as energy storage systems in portable electronics and electric vehicles [1-3]. Nevertheless, the energy density of commercial LIBs cannot meet the increasing requirements for electrical vehicles and renewable sources of energy. At present, graphite-type carbon materials outperform LIB anode materials [4-7]. However, the theoretical capacity of graphite is rarely 372 mAh g⁻¹ [8], which severely limits the development of high-energy LIBs. To improve the energy density, non-carbon anode materials such as metal oxides [9-13], alloys [14-16], and silicon [17-22] have been investigated owing to their high specific capacity.

However, the large volume variation of these anode materials causes rapid decay of the battery capacity during the process of Li^+ insertion and extraction [23], which in turn affects the cycling stability of the battery. At the same time, the synthesis of those kinds of non-carbon anode materials is a high-energy consumption process, and the application of transition metals leads to severe resource and environmental problems [24]. In addition, the inorganic anode materials on the market today have had difficulty meeting the growing demand for battery capacity. Therefore, researchers have begun to explore environmentally friendly organic anode materials with a flexible design and low energy consumption in order to meet the ambitious requirements for new battery anode materials [25].

Over the last ten years or more, several types of organic materials, such as aromatic carbonyl derivatives [26-28], conductive polymers [29-31], polyimide [32-34], etc., have been reported as electrodes for LIBs. However, many challenges still exist in developing organic anode materials with excellent electrochemical performance. To avoid the dissolution of organic materials in the electrolyte and to obtain fast reaction kinetics, the selected organic material must have a stable skeleton [25]. Additionally, the organic electrode material should have a large π -conjugated structure for better electron transportation in the electrode of LIBs. A π -conjugated structure is beneficial to the fast charge transfer, reducing the resistance of the battery.

Iron-phthalocyanine (FePc), a metal-organic compound containing large π -conjugated and a planar multi-ring aromatics structure [35, 36], is considered an intriguing candidate for LIBs. In the late 80s, Yamaki et al. investigated the electrochemical reaction mechanism of a FePc electrode and concluded that Li^+ could be intercalated and de-intercalated electrochemically among the large planar FePc molecules [37]. Later, Crowther et al. reported FePc as a cathode in a primary lithium (Li) battery and achieved a high capacitance of 2050 mAh g^{-1} , which corresponds to the insertion of 43 Li^+ for each FePc molecule based on an electrode with 25% nanographene (NGP) [38]. According to recent reports [39-40], redox reactions could relatively easily occur on unsaturated atoms with a lone electron pair, such as unsaturated nitrogen or oxygen atoms, even on unsaturated carbon atoms, such as aromatic carbon rings. Then, each aromatic C_6 ring could reversibly accept six lithium ions to form a Li_6/C_6 compound [39]. In this case, the FePc has a theoretical storage capacity of 1792 mAh g^{-1} , which corresponds to an insertion of 38 Li^+ for each FePc molecule, which is less than the insertion of 43 Li^+ for each FePc, as mentioned above [38]. The unexpected higher storage capacity may originate from a π -conjugated structure of FePc with an interlayer spacing of 0.34 nm, which is extremely close to the interlayer distance of graphite (0.3354 nm) [8, 35], a suitable gap size for the insertion and extraction of lithium ions during the discharge/charge process of LIBs. This is a very interesting phenomenon, deserving further exploration in secondary batteries.

As we know, the electronic conductivity of iron-phthalocyanine is poor; although, there is a large π -conjugated molecular structure with a high-density electron cloud. Furthermore, graphene nanosheets (GNs), two-dimensional carbon nanomaterials, have aroused widespread attention due to their superior intrinsic properties, especially their high electronic conductivity and flexibility. Its excellent properties render graphene an excellent electrode material for LIBs [40-42]. Such an electrode material has a high specific capacity as well as an excellent electrical conductivity. However, graphene is so expensive that it can only be used as an additive to improve the conductivity of the electrode with the aim of improving the rate performance of the battery.

In this work, we presented a strategy of preparing a high-performance electrode for secondary Li-ion batteries by blending FePc and GN in different proportions to fabricate organic/inorganic composites of FePc and GN. Thus, graphene not only acts as a conducting agent but also as an active material in the electrodes. At the same time, the large quantity of graphene mixed in FePc creates many interfacial gaps, which provide many channels for the penetration of electrolyte in the electrode, facilitating the diffusion of Li ions in the electrode and improving the rate performance of the electrode. Electrochemical tests showed that the as-prepared composite electrode with FePc/GN=1/2.25 reached a high reversible capacity of 847 mAh g⁻¹, which suggests that the storage capacity of FePc is up to 1614 mAh g⁻¹ in the composite electrode.

2. EXPERIMENTAL

2.1. Electrode preparation

The FePc/GN composite was prepared by blending iron-phthalocyanine powder (J&K) and graphene nanosheets in different weight ratios. The graphene sheets were synthesized via a solvothermal method reported previously [43]. Typically, we controlled the ratio of FePc weight to 1 and changed the GN weight ratio from 1.25 to 2.75. The obtained composites were denoted as 1/1.25-FePc/GN, 1/1.75-FePc/GN, 1/2.25-FePc/GN, 1/2.5-FePc/GN, 1/2.75-FePc/GN, respectively. Then, the FePc/GN composites were mixed with a binder polyvinylidene difluoride (PVDF) in a weight ratio of FePc/GN/PVDF=9:1 using N-methyl pyrrolidinone (NMP, Aldrich) as a dissolving solvent. The mixture was stirred to form a homogeneous slurry, which was then casted onto a copper foil as the current collector. The copper foil coated with the slurry was dried at 100°C for 6 hours and then cut into circular disks as test electrodes. Lithium foil was used as a counter electrode, the electrolyte was a solution of 1 M LiPF₆ in diethyl carbonate (DEC)/ethylene carbonate (EC)/dimethyl carbonate (DMC) (1:1:1 in volume), and the separator was a Celgard 2300 micro-porous membrane. These above materials were assembled together with the test electrodes to obtain coin cells in an argon-filled glove box.

2.2. Electrochemical measurement

The phase structures of FePc were analysed by using an X-ray diffraction system (XRD, Siemens 5000). The cyclic voltammetry (CV) tests were carried out on an electrochemical workstation (EC-lab VMP3, Bio-logic, France) over a potential range from 0.01 to 3.0 V vs. Li/Li⁺ at a scanning rate of 0.1 mV s⁻¹. The galvanostatic charge and discharge was in the voltage range from 0.01 to 3.0 V (vs. Li/Li⁺) using a multi-channel battery testing system (LAND-CT2001A, Wuhan Jinnuo, China). Rate capacity studies were performed ranging from 300 to 2000 mA g⁻¹.

3. RESULTS AND DISCUSSION

The scanning electron microscope (SEM) image in Fig. 1a shows that the FePc powder is composed of rice grain-like nanoparticles. The magnified SEM image (Fig. 1b) reveals that the densely packed nanograins have a length in the range of 40-80 nm. The transmission electron microscopy (TEM) image (Fig. 1c) further shows that the FePc nanoparticles have a rice grain-like shape with a smooth surface. The yellow selected areas in the TEM image (Fig. 1c) are respectively magnified in Fig. 1d and 1e, in which a lattice fringe spacing of 1.26, 0.57 and 0.35 nm can be correspondingly ascribed to the (200), (-402) and (-211) crystalline planes. The XRD pattern shows that the FePc used in this work is a meta-stable α -polymorph. The peaks at 6.9, 9.9, 15.7° correspond to the (200), (-202) and (-402) crystalline planes of the meta-stable α -polymorph (JCPDS Card NO.22-1771) [35]. It is also observed for the diffuse halo range from 23 to 26°, which appears at the maxima of the (011) and (-211) reflections of the FePc α -polymorph (Fig. 1f).

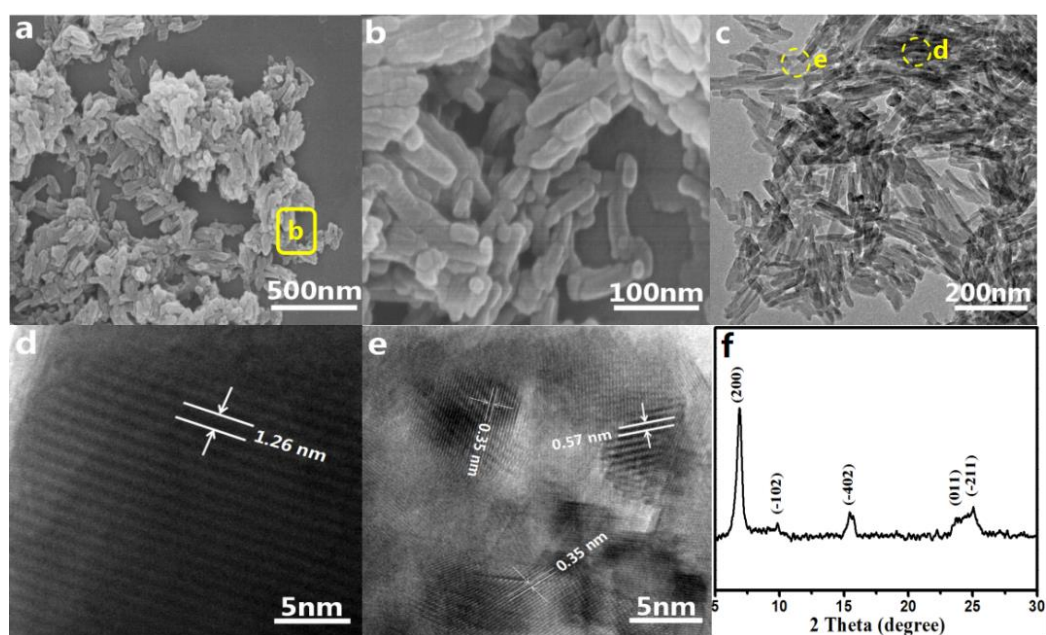


Figure 1. SEM and TEM images and X-ray pattern of the iron-phthalocyanine powder: low (a) and high (b) magnification SEM images; TEM (c) and HR-TEM (d, e) images; X-ray diffraction pattern (f).

The reversibility and kinetics of Li intercalation and de-intercalation in the FePc/GN composites were studied using cyclic voltammetry. Fig. 2 shows the representative CV curves of the composite 1/2.25-FePc/GN scanned from 3.0 to 0.01 V versus a Li/Li⁺ reference electrode at a rate of 0.1 mV s⁻¹. The lithium-ion insertion potential was approximately 0.17 V for graphene in the composite electrode, and the corresponding de-intercalation potential was approximately 0.2 V [44]. A larger broad reduction peak was observed at approximately 0.75 V, which can be attributed to the lithiation of FePc molecules on the carbon of C₆ aromatic rings and the formation of a solid electrolyte interphase (SEI) film at the electrode-electrolyte interface [45]. Broad peaks at the potential of

approximately 1.52 V are associated with the addition of lithium to unsaturated nitrogen [31, 45]. Meanwhile, a corresponding broad anodic peak observed at approximately 1.0-1.6 V in the reverse sweep can be identified as the delithiation process. Compared to the second cycle, no significant change occurs in the third cycle onward, which indicates that the electrode is relatively stable and highly reversible in the delithiation reaction.

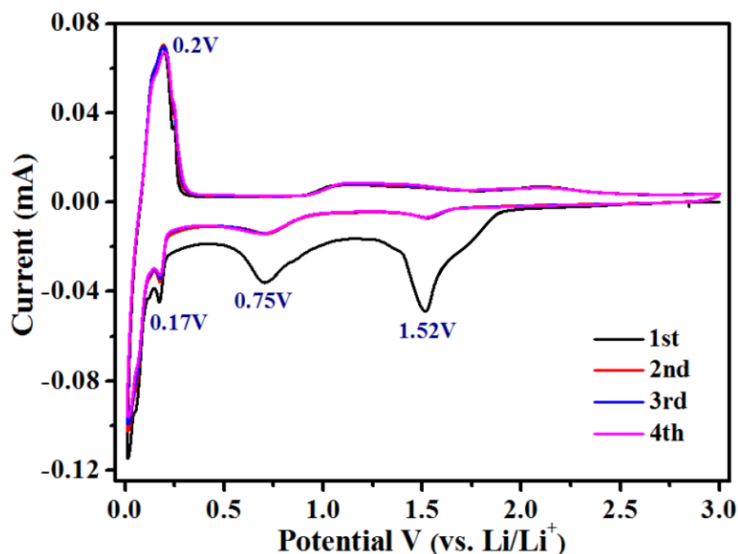


Figure 2. Cycle voltammetry profiles of 1/2.25-FePc/GN composite.

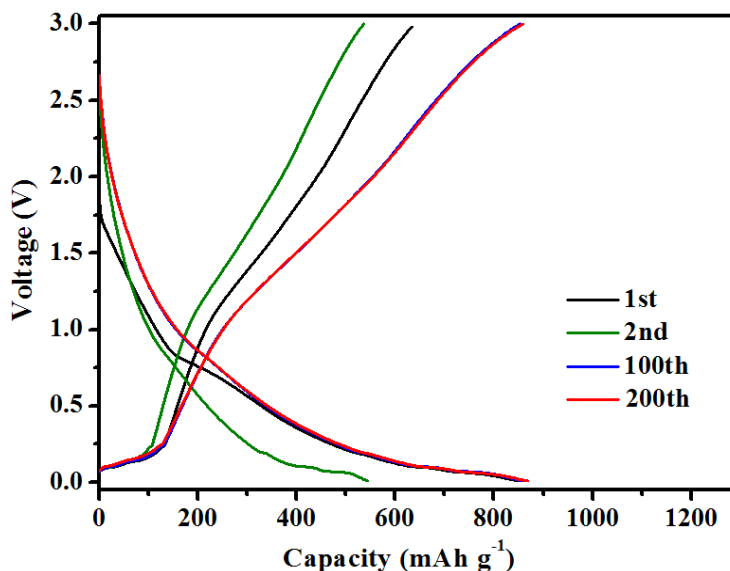


Figure 3. Charge and discharge curves at the 1st, 2nd, 100th, 200th cycles of 1/2.25-FePc/GN composite at a current density of 300 mA g⁻¹.

The galvanostatic charge-discharge tests of the 1/2.25-FePc/GN composite electrode were performed at a current density of 300 mA g⁻¹. As shown in Fig. 3, the first discharge and charge capacities are found to be 849.2 and 633.7 mAh g⁻¹. The lower initial coulombic efficiency (74.6%) is attributed to the irreversible capacities from the formation of the SEI film, which is a common

characteristic of LIB anodes in the first cycle [46, 47]. The second discharge and charge capacities are 851 and 838 mAh g⁻¹ with a coulombic efficiency of 98.5%, which substantially reduced the reversible capacity loss. Apparently, in the discharging profile of the first cycle, the well-defined plateau at 0.75 V can be attributed to the lithiation of the FePc molecules on the carbon of the C₆ aromatic rings. For our FePc/GN composite anode, the specific discharge capacity from 0.01 to 3 V is 541, 857.6 and 872.8 mA h g⁻¹ at the 2nd, 100th and 200th cycle, respectively, suggesting that the insertion of Li ions into FePc is highly reversible before 200 cycles. The capacity increases are mainly caused by the activation phenomenon of the electrode materials with more reaction sites during the charge/discharge process.

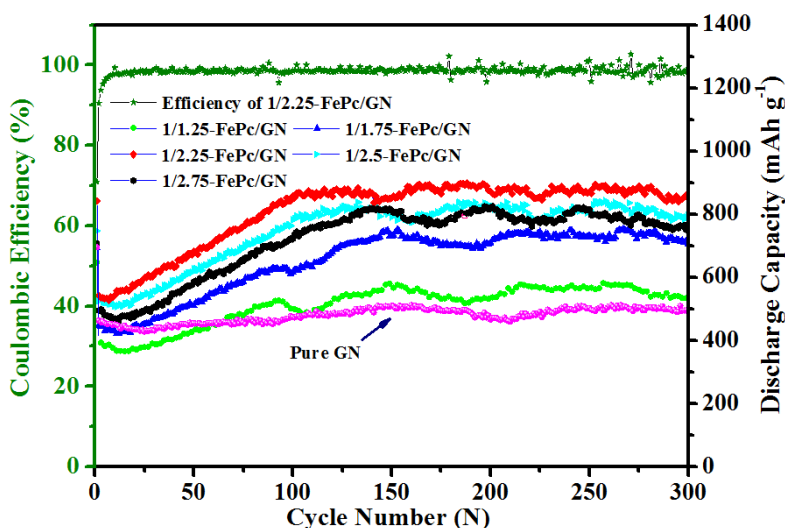


Figure 4. Cycle performance of FePc/GN in different weight ratios and pure GN at a current density of 300 mA g⁻¹.

The capacity of FePc/GN composites in different ratios at a current density of 300 mA g⁻¹ are shown in Fig. 4. Surprisingly, the specific capacity continues to increase and then basically remains constant after the first 100 cycles. Among them, the 1/2.25-FePc/GN composite obtains an optimal capacity of 873 mAh g⁻¹, which is 2.5 times higher than the theoretical capacity of commercial graphite (372 mAh g⁻¹). Fast capacity fading is observed for the first twenty cycles. Thereafter, the capacity remains increased for the subsequent cycles. The increase in the reversible capacity is believed to be a gradual activation process [10, 48-50], but this phenomenon does not occur for GN.

The rate performance of the composite 1/2.25-FePc/GN is presented in Fig. 5. As the current rates increase from 300 to 500, 750, 1000, 1500, and 2000 mA g⁻¹, the 1/2.25-FePc/GN electrode exhibits a superior capacity retention of 847, 757, 664, 559, 466, and 351 mAh g⁻¹, respectively. Relative to the maximum capacity of 847 mAh g⁻¹ at 300 mA g⁻¹, the capacity retention is 89%, 78%, 65%, 55%, and 41% at an increased current density of 500, 750, 1000, 1500, and 2000 mA g⁻¹, respectively. When the current density decreased from 2000 to 300 mA g⁻¹, the capacity also recovered to 845 mAh g⁻¹, indicating the excellent rate stability and reversibility of the 1/2.25-FePc/GN

electrode. For organic electrode materials, the high capacity and good rate performance described above have been rarely reported in the past.

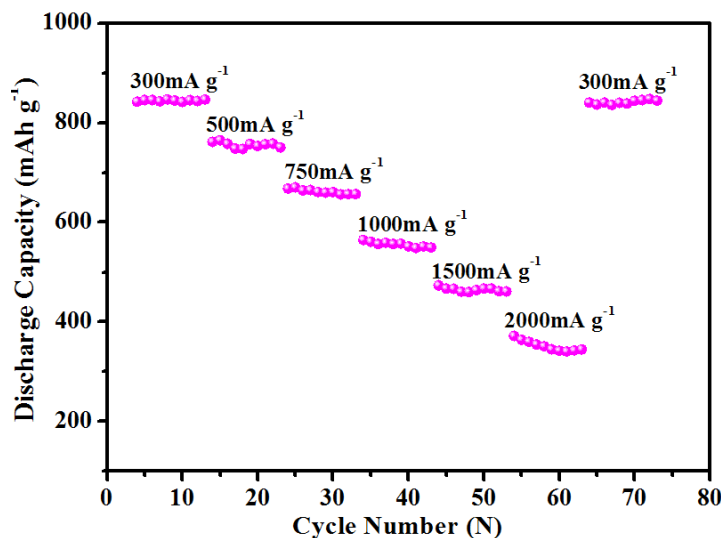


Figure 5. Cycling performance of 1/2.25-FePc/GN composite at various current densities between 300 and 2000 mA g⁻¹.

Table 1. The capacity contribution of FePc and GN at different weight ratios.

Weight ratio of FePc/GN (N/N)	The capacity of FePc/GN (mAh g ⁻¹) (C _N)	The capacity of GN (mAh g ⁻¹) (C _B)	The capacity of FePc (mAh g ⁻¹) (C _A)
1:1.25	539	509	606
1:1.75	706	509	1149
1:2.25	849	509	1614
1:2.50	796	509	1441
1:2.75	766	509	1344

The contribution capacity of FePc was calculated by the following equation:

$$C_N = C_A \times W_A + C_B \times W_B \quad (1)$$

where C_N is the capacity of the FePc/GN composite, C_A is the specific capacity based on FePc, C_B is the specific capacity based on GN, W_A is the weight ratio of FePc, and W_B is the weight ratio of GN. According to Fig. 2 and equation (1), the specific capacity based on FePc at different proportions in the FePc/GN composite was calculated and recorded in Table 1. It can be seen that the composite electrode exhibits a lower discharge capacity when the graphene content in the FePc/GN composite was lower or higher than a mass ratio of 1:2.25. As we know, the FePc is an organic material with a poor electronic conductivity. Thus, the FePc in the composite cannot be fully used due to the hampering of charge transfer in the electrode system at a lower graphene content. As a result, the capacity of the composite electrode is lower than that of the electrode with a mass ratio of 1:2.25. Furthermore, the composite electrode also gives a lower capacity at a higher graphene content. This may originate from a lower storage capacity of graphene compared to the capacity of FePc. By Fig. 6,

it is obvious that the specific capacity based on FePc first increases with the increase of graphene content, and then reaches its maximum at a critical value of graphene content (1:2.25 in weight). Then, the curve shows a slight drop in the horizontal line with a continuous increase in the graphene content. The optimal capacity of FePc in the composite electrode reaches 1614 mAh g^{-1} , as calculated by equation (1) above using the maximum of the capacity of the FePc/GN composite.

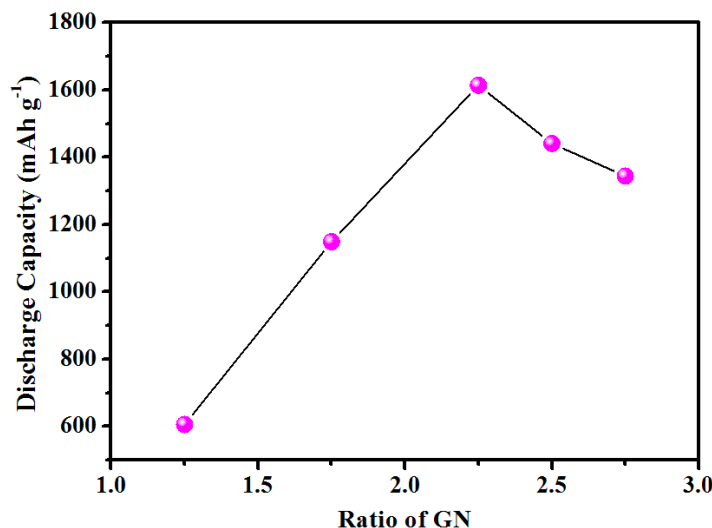
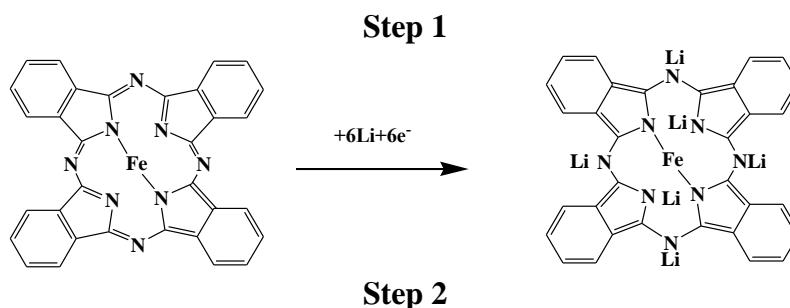
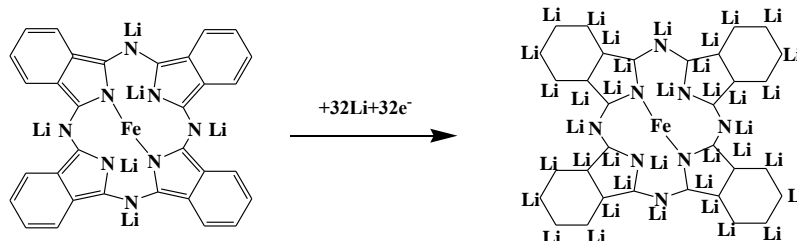


Figure 6. The specific capacity based on FePc at different weight ratios in the composites.

Theoretically, there are 19 unsaturated double bonds in the iron-phthalocyanine molecule, wherein each unsaturated double bond can undergo the addition reaction with lithium ion and reversibly accept two lithium ions. Thus, the C_6 aromatic rings can accept six lithium ions to form a Li_6/C_6 complex [35, 39, 45]. Additionally, there are six $C=N$ unsaturated double bonds in the iron-phthalocyanine molecule, redox reactions can first occur on the nitrogen atom with a lone pair of electrons [31, 45]. The following **step 1** illustrates the addition of the lithium ion to the unsaturated nitrogen, and six lithium ions are reversibly accepted in this process; **step 2** shows the lithiation of FePc molecules on the carbons of C_6 aromatic rings and on the unsaturated $C=C$ double bonds of the pyrrole rings, and 32 lithium ions are reversibly accepted in the second process. In summary, each iron-phthalocyanine molecule can reversibly accept 38 lithium ions in total.





Thus, we can calculate the specific capacity of FePc by the following formula :

$$C_l = 26802 \times n / M \quad (2)$$

where C_l is the specific capacity of FePc based on the lithiation of 38 Li ions, n is the acceptable number of electrons, and M is the molecular weight of FePc ($M=568.37$). That is, $C_l = 26802 \times 38 / 568.37 = 1792 \text{ mAh g}^{-1}$. Experimentally, we obtained a 1614 mAh g^{-1} maximum of the FePc capacity, which is very close to the theoretical capacity.

4. CONCLUSIONS

FePc/GN composites, as high-electrochemical-performance organic electrode materials, were prepared by mixing organic-metal complex FePc and highly conductive graphene (GN) in the dispersant NMP. The FePc/GN composite with a weight ratio of FePc/GN=1/2.25 (1/2.25-FePc/GN) had a high capacity of 847 mAh g^{-1} at a current density of 300 mA g^{-1} and 351 mAh g^{-1} at 2000 mA g^{-1} , showing a good rate performance. The specific capacity based on FePc was calculated to be as high as 1614 mAh g^{-1} at a current density of 300 mA g^{-1} based on the weight ratio of 1/2.25. Such excellent electrochemical performance is attributed to the large π -conjugated structure, rich N atoms with one electron pair and the aromatic rings in the FePc molecule as well as the interlayer structure of FePc. At last, this work provided important insight into developing a new generation of organic anode materials for high-performance LIBs, and such organic/inorganic composite materials may find broad applications in the future field of secondary batteries.

ACKNOWLEDGEMENTS

This research was supported by the National Natural Science Foundation of China (Grants No.: 21774053); the Major Special Projects of Jiangxi Provincial Department of Science and Technology (Grant No.: 20114ABF05100) and the Technology Plan Landing Project of Jiangxi Provincial Department of Education (Grant No.: KJLD1104).

References

1. J.B. Goodenough, Y. Kim, *Chem. Mater.* 22 (2010) 587-603.
2. X. Rui, X. Zhao, Z. Lu, H. Tan, D. Sim, H.H. Hng, R. Yazami, T.M. Lim, Q. Yan, *ACS Nano*, 7 (2013) 5637-5646.
3. Z. Zhu, S. Wang, J. Du, Q. Jin, T. Zhang, F. Cheng, J. Chen, *Nano Lett.* 14 (2014) 153-157.
4. A.K. Padhi, K.S. Nanjundaswamy, J.B. Goodenough, *J. Electrochem. Soc.*, 144 (1997) 1188-1194.
5. [5] J.R. Dahn, T. Zheng, Y. Liu, J.S. Xue, *Science*, 270 (1995) 590-593.

6. K. Sawai, Y. Iwakoshi, T. Ohzuku, *Solid State Ion.* 69 (1994) 273-283.
7. D.S. Su, R. Schlogl, *ChemSusChem*, 3 (2010) 136-168.
8. K. Tatsumi, *J. Electrochem. Soc.* 142 (1995) 716.
9. P. Lian, X. Zhu, S. Liang, Z. Li, W. Yang, H. Wang, *Electrochim. Acta*, 56 (2011) 4532-4539.
10. L. Liu, H. Zhang, S. Liu, H. Yao, H. Hou, S. Chen, *Electrochim. Acta*, 219 (2016) 356-362.
11. M. Lübke, N. Ding, M.J. Powell, D.J.L. Brett, P.R. Shearing, Z. Liu, J.A. Darr, *Electrochem. Commun.* 64 (2016) 56-60.
12. Z.-S. Wu, G. Zhou, L.-C. Yin, W. Ren, F. Li, H.-M. Cheng, *Nano Energy*, 1 (2012) 107-131.
13. A.K. Rai, L.T. Anh, J. Gim, V. Mathew, J. Kang, B.J. Paul, N.K. Singh, J. Song, J. Kim, *J Power Sources*, 244 (2013) 435-441.
14. C.M. Park, J.H. Kim, H. Kim, H.J. Sohn, *Chem. Soc. Rev.* 39 (2010) 3115-3141.
15. J. Cabana, L. Monconduit, D. Larcher, M.R. Palacin, *Adv. Mater.* 22 (2010) E170-192.
16. L. Ji, Z. Lin, M. Alcoutlabi, X. Zhang, *Energy & Environ. Sci.* 4 (2011) 2682.
17. S.-L. Chou, J.-Z. Wang, M. Choucair, H.-K. Liu, J.A. Stride, S.-X. Dou, *Electrochem. Commun.* 12 (2010) 303-306.
18. Y.S. Hu, R. Demir-Cakan, M.M. Titirici, J.O. Muller, R. Schlogl, M. Antonietti, J. Maier, *Angew. Chem. Int. Ed.* 47 (2008) 1645-1649.
19. H. Xiang, K. Zhang, G. Ji, J.Y. Lee, C. Zou, X. Chen, J. Wu, *Carbon*, 49 (2011) 1787-1796.
20. Y. Yao, M.T. McDowell, I. Ryu, H. Wu, N. Liu, L. Hu, W.D. Nix, Y. Cui, *Nano Lett.* 11 (2011) 2949-2954.
21. X. Zhou, Y.X. Yin, L.J. Wan, Y.G. Guo, *Chem. Commun.* 48 (2012) 2198-2200.
22. L. Zhu, H.Q. Hou, D. Zhao, S.W. Liu, W. Ye, S.L. Chen and M. Hanif, *Int. J. Electrochem. Sci.*, 10 (2015) 9547-9555.
23. Y. Piao, H.S. Kim, Y.E. Sung, T. Hyeon, *Chem. Commun.* 46 (2010) 118-120.
24. P. Poizot, F. Dolhem, *Energy & Environ. Sci.* 4 (2011) 2003.
25. Z. Song, H. Zhou, *Energy & Environ. Sci.* 6 (2013) 2280.
26. A.J. Wain, G.G. Wildgoose, C.G. Heald, L. Jiang, T.G. Jones, R.G. Compton, *J. Phys. Chem. B*, 109 (2005) 3971-3978.
27. X. Han, C. Chang, L. Yuan, T. Sun, J. Sun, *Adv. Mater.* 19 (2007) 1616-1621.
28. Y. Liang, P. Zhang, S. Yang, Z. Tao, J. Chen, *Adv. Energy Mater.* 3 (2013) 600-605.
29. P. Gomez-Romero, *Adv. Mater.* 13 (2001) 163-174.
30. T. Sun, Z.J. Li, H.G. Wang, D. Bao, F.L. Meng, X.B. Zhang, *Angew. Chem. Int. Ed.* 55 (2016) 10662-10666.
31. K. Sakaushi, G. Nickerl, F.M. Wisser, D. Nishio-Hamane, E. Hosono, H. Zhou, S. Kaskel, J. Eckert, *Angew. Chem. Int. Ed.* 51 (2012) 7850-7854.
32. F. Xu, J. Xia, W. Shi, S.-a. Cao, *Chem. Lett.* 45 (2016) 271-273.
33. L. Chen, W. Li, Y. Wang, C. Wang, Y. Xia, *RSC Adv.* 4 (2014) 25369-25373.
34. Z. Song, H. Zhan, Y. Zhou, *Angew. Chem. Int. Ed.* 49 (2010) 8444-8448.
35. Adriyan S. Milev, Nguyen Tran, G. S. Kamali Kannangara, a. Michael A. Wilson, A. Isak, *J. Phys. Chem. C*, 112 (2008) 5339-5347.
36. C.G. Barraclough, R.L. Martin, S. Mitra, R.C. Sherwood, *J. Chem. Phys.* 53 (1970) 1643-1648.
37. S. Okada, J.I. Yamaki, *J. Electrochem. Soc.* 136 (1989) 2437-2440.
38. O. Crowther, L.-S. Du, D.M. Moureau, I. Bicaku, M. Salomon, J.W. Lawson, L.R. Lucente, K. Mock, J.P. Fellner, L.G. Scanlon, *J. Power Sources*, 217 (2012) 92-97.
39. X. Han, G. Qing, J. Sun, T. Sun, *Angew. Chem. Int. Ed.* 51 (2012) 5147.
40. P. Guo, H. Song, X. Chen, *Electrochem. Commun.* 11 (2009) 1320-1324.
41. X. Huang, X. Qi, F. Boey, H. Zhang, *Chem. Soc. Rev.* 41 (2012) 666-686.
42. P. Lian, X. Zhu, S. Liang, Z. Li, W. Yang, H. Wang, *Electrochim. Acta*, 55 (2010) 3909-3914.
43. M. Choucair, P. Thordarson, J.A. Stride, *Nat. nanotech.* 4 (2009) 30-33.
44. K. Rana, S.D. Kim, J.H. Ahn, *Nanoscale*, 7 (2015) 7065-7071.

45. J. Wu, X. Rui, C. Wang, W.-B. Pei, R. Lau, Q. Yan, Q. Zhang, *Adv. Energy Mater.* 5 (2015) 1402189.
46. J. Luo, J. Liu, Z. Zeng, C.F. Ng, L. Ma, H. Zhang, J. Lin, Z. Shen, H.J. Fan, *Nano Lett.* 13 (2013) 6136-6143.
47. E. Kang, Y.S. Jung, A.S. Cavanagh, G.-H. Kim, S.M. George, A.C. Dillon, J.K. Kim, J. Lee, *Adv. Funct. Mater.* 21 (2011) 2430-2438.
48. C. Peng, B. Chen, Y. Qin, S. Yang, C. Li, Y. Zuo, S. Liu, J. Yang, *ACS Nano*, 6 (2012) 1074.
49. Y. Sun, X. Hu, W. Luo, F. Xia, Y. Huang, *Adv. Funct. Mater.* 23 (2013) 2436-2444.
50. F. Zou, X. Hu, Z. Li, L. Qie, C. Hu, R. Zeng, Y. Jiang, Y. Huang, *Adv. Mater.* 26 (2014) 6622-6628.

© 2018 The Authors. Published by ESG (www.electrochemsci.org). This article is an open access article distributed under the terms and conditions of the Creative Commons Attribution license (<http://creativecommons.org/licenses/by/4.0/>).